

# Changes in brain functional connectivity patterns are driven by an individual lesion in MS: a resting-state fMRI study

Amgad Droby<sup>1,2</sup> · Kenneth S. L. Yuen<sup>2</sup> · Muthuraman Muthuraman<sup>1,2</sup> · Sarah-Christina Reitz<sup>3,4</sup> · Vinzenz Fleischer<sup>1</sup> · Johannes Klein<sup>3,4</sup> · René-Maxime Gracien<sup>3,4</sup> · Ulf Ziemann<sup>5</sup> · Ralf Deichmann<sup>4</sup> · Frauke Zipp<sup>1,2</sup> · Sergiu Groppa<sup>1,2</sup>

**Abstract** Diffuse inflammation in multiple sclerosis (MS) extends beyond focal lesion sites, affecting interconnected regions; however, little is known about the impact of an individual lesion affecting major white matter (WM) pathways on brain functional connectivity (FC). Here, we longitudinally assessed the effects of acute and chronic lesions on FC in relapsing-remitting MS (RRMS) patients using resting-state fMRI. 45 MRI data sets from 9 RRMS patients were recorded using 3T MR scanner over 5 time points at 8 week intervals. Patients were divided into two groups based on the presence ( $n=5$ ; MS+) and absence ( $n=4$ ; MS-) of a lesion at a predilection site for MS. While FC levels were found not to fluctuate significantly in the overall patient group, the MS+ patient group showed increased FC in the contralateral cuneus and precuneus and in the ipsilateral precuneus ( $p < 0.01$ ,

corrected). This can be interpreted as the recruitment of intact cortical regions to compensate for tissue damage. During the study, one patient developed an acute WM lesion in the left posterior periventricular space. A marked increase in FC in the right pre-, post-central gyrus, right superior frontal gyrus, the left cuneus, the vermis and the posterior and anterior lobes of the cerebellum was noted following the clinical relapse, which gradually decreased in subsequent follow-ups, suggesting short-term functional reorganization during the acute phase. This strongly suggests that the lesion-related network changes observed in patients with chronic lesions occur as a result of reorganization processes following the initial appearance of an acute lesion.

**Keywords** Compensation · Functional connectivity · Neuroplasticity · rs-fMRI

---

Frauke Zipp and Sergiu Groppa contributed equally to this work.

✉ Sergiu Groppa  
sergiu.groppa@unimedizin-mainz.de

- <sup>1</sup> Department of Neurology, University Medical Centre of the Johannes Gutenberg University Mainz, Mainz, Germany
- <sup>2</sup> Neuroimaging Center (NIC) of the Focus Program Translational Neuroscience (FTN), Johannes Gutenberg University Mainz, Langenbeckstr. 1, 55131 Mainz, Germany
- <sup>3</sup> Department of Neurology, University Hospital Frankfurt, Frankfurt am Main, Germany
- <sup>4</sup> Brain Imaging Center (BIC), Goethe University, Frankfurt am Main, Germany
- <sup>5</sup> Department of Neurology and Stroke, Hertie Institute for Clinical Brain Research, Eberhard-Karls-University, Tübingen, Germany

## Introduction

Multiple sclerosis (MS) is an inflammatory demyelinating disease of the central nervous system (CNS), and magnetic resonance imaging (MRI) serves as a key tool in its diagnosis and in monitoring the disease course and treatment outcomes (Polman et al. 2011; Filippi et al. 2012; Rovira et al. 2013; Bremel and Naismith 2015). However, studies applying conventional MRI sequences have failed to report strong correlations between white matter (WM) damage and gray matter (GM) atrophy in MS (De Stefano et al. 2002; Calabrese et al. 2015). Conventional MRI is highly sensitive for the detection of demyelinating lesions, but diffuse subtle WM damage can only be monitored indirectly. Thus, determining the impact of acute and chronic lesions on distant cortical areas and associated changes of connectivity in affected

regions remains challenging (Rovaris et al. 1999; Chard and Miller 2009; Droby et al. 2015).

Resting-state functional MRI (rs-fMRI) can be employed to depict functional connectivity (FC) dynamics over the disease course, and thus better reflect the association between evolving tissue pathology and clinical disability (Faivre et al. 2012). With the aid of rs-fMRI, spontaneous brain activity can be analyzed and integrated into longitudinal analyses of network dynamics, which could give a better temporal and spatial description of chronic and acute disease process (Fox and Raichle 2007). Several earlier studies have reported FC pattern changes in patients with MS in comparison to healthy controls (Rocca et al. 2010; Dogonowski et al. 2012; Dogonowski et al. 2013; Basile et al. 2013; Gamboa et al. 2014). Focusing on functional motor network connectivity in MS patients at rest, Dogonowski et al. (2012) reported stronger functional integration of the basal ganglia and thalamus into the motor network in these patients compared to healthy controls. The increase in FC in these brain regions was found to be independent of clinical features and MR structural measures of the studied patient group.

In relapsing-remitting MS (RRMS) patients, however, an FC increase was hypothesized to compensate for ongoing damage during the initial disease stages (Faivre et al. 2012; Basile et al. 2013). An FC increase in frontal regions was observed to facilitate performance in complex speed-dependent information processing tasks (Wojtowicz et al. 2014). Basile et al. (2013) have reported that FC increases within both the default mode network (DMN) and sensory-motor network (SMN) in RRMS patients at rest compared to healthy controls, arguing that these changes correlate with the patient's ability to compensate for functional disability. Zhou et al. (2014) were able to demonstrate a connection between WM abnormalities as depicted by diffusion tensor imaging (DTI) and functional damage in RRMS patients using rs-fMRI. Employing DTI tractography together with rs-fMRI, they reported significantly reduced pairwise structural connections and increased FC in distant sub-regions of the DMN in RRMS patients compared to healthy controls. The applicability of these rs-fMRI studies of RRMS to the general MS population is limited, however, since the majority of these studies focus on several resting-state networks such as the DMN, and they do not account for the direct impact of the local distribution of WM lesions and GM volume (Ceccarelli et al. 2008; Rocca et al. 2012). Moreover, inflammatory lesions are distributed throughout the brain in MS and are not restricted solely to the DMN (Richiardi et al. 2012).

Individual MS lesions affecting major WM pathways may induce global network connectivity changes (Droby et al. 2015). Evidence for the impact of a single typical MS lesion on FC changes has been reported by Jones et al. (2011). In a case study based on a 40-year-old male presenting with a gadolinium-enhancing lesion at the anterior thalamus, rs-

fMRI revealed alterations in DMN circuitry that was attributed to this lesion, while FC in the posterior cingulate cortex (PCC), precuneus and the left inferior parietal lobe was reduced compared to healthy controls (Jones et al. 2011).

In this study, we investigate the impact of a single lesion in the left posterior periventricular space, an area frequently affected by MS plaques (Polman et al. 2011), on brain resting-state FC. The main objectives of this work are to determine (i) network FC changes over time; (ii) longitudinal spatial alterations in FC levels between two groups of MS patients with and without a lesion at this predilection site; and (iii) alterations of FC in patients with an acute demyelinating inflammatory lesion at this predilection site.

## Methods

### Participants

Nine RRMS patients (six females, age [mean±SD]=40.1±13 years, disease duration (DD)=3.7±6 years, expanded disability status-scale (EDSS) score at baseline [median, range]=1.5, 0–2.5) were included in the study. Four showed chronic lesions in either the left ( $N=1$ ) or right ( $N=3$ ) posterior periventricular region, as indicated by a hyperintense signal in T2-FLAIR images and hypointense signal in T1 images (MS+ group; mean age=42.8±9.2; DD=6.2±8). The remaining patients showed no similar lesion (MS-; mean age=41.8±9.16; DD=1±0.33). No significant clinical or demographic differences were detected between the MS+ and MS- patients groups in age, DD or EDSS scores (two-sample  $t$ -test; Age:  $T=0.18$ ,  $p=0.86$ ; DD:  $T=1.3$ ,  $p=0.23$  and EDSS: Mann-Whitney  $U$ -test=7,  $p=0.45$ ). An overview of the clinical data of the included patients is given in Table 1. All patients gave their informed consent to participate in this study, which was approved by the local ethics committee.

During the study period, a single patient (32-year-old female; age at disease onset, 27; DD=5 years; EDSS=1 at inclusion) developed a new WM lesion in the left posterior periventricular region. This allowed investigation of the impact of a new lesion on FC changes over time. No further subjects in the studied patient sample developed new inflammatory lesions during the follow-up period.

### MRI protocol

MR data was acquired for all patients using a 3T MR scanner (Magnetom TimTrio<sup>®</sup>, Siemens, Germany) with a 32-channel head coil and using the following protocol: 3D T1-weighted MP-RAGE sequence (TI=900 ms, TR=1900 ms, TE=2.52 ms, FOV=256×265 mm<sup>2</sup>, flip angle=9°, voxel size=1×1×1 mm<sup>3</sup>, 192 sagittal slices, 16.7 % slice oversampling to avoid aliasing, receiver band width=170 Hz/pixel,

**Table 1** Clinical data for the studied RRMS patients

Patient code	Gender	Disease course	Age of onset (years)	Age at inclusion (years)	Disease duration (months)	EDSS at baseline	T2-lesion load at baseline (mm <sup>3</sup> )	Treatment
Pat_1	Female	CIS	20	21	12	0	0	Immunomodulating drug
Pat_2	Female	RRMS	52	54	18	1	0.4	Immunomodulating drug
Pat_3	Female	RRMS	61	61	4	1.5	1	naïve
Pat_4	Female	RRMS	26	33	76	1	10.20	Monoclonal antibodies
Pat_5	Male	RRMS	24	44	240	2	5.7	naïve
Pat_6	Male	RRMS	32	34	18	1	10	Monoclonal antibodies
Pat_7	Female	RRMS	43	44	4	2.5	0.6	Immunomodulating drug
Pat_8	Male	RRMS	49	49	2	1.5	5.3	Immunomodulating drug
Pat_9	Female	RRMS	38	38	4	2	0.5	naïve

duration=4:26 min). 3D T2-weighted TSE sequence with fluid suppression (FLAIR), (TR=5000 ms, TE=389 ms, TI=1800 ms, FOV=256×256 mm<sup>2</sup>, flip angle=120°, voxel size=1×1×1 mm<sup>3</sup>, 192 sagittal slices, band width=781 Hz/pixel, duration 8:02 min). The diffusion data were obtained using a diffusion-weighted spin echo EPI sequence (TR=9000 ms, TE=102 ms, 30 diffusion-encoding gradient directions,  $b=0$  and 900 s/mm<sup>2</sup>, FOV=256×256 mm<sup>2</sup>, matrix size=128×128, flip angle=90°, 62 axial slices with a slice thickness of 2 mm and an inter-slice gap=0.5 mm, voxel size=2×2 mm<sup>2</sup>, number of averages=1, band width=2056 Hz/pixel, echo spacing=0.78 ms, duration=5:08 min). rs-fMRI data were obtained using a gradient echo EPI sequence (TR=3000 ms, TE=30 ms, flip angle=90°, a matrix size of 64×64, spatial in-plane resolution of 3 mm, 49 axial slices with a slice thickness of 2 mm and an inter-slice gap of 1 mm, band width=2232 Hz/pixel, echo spacing=0.51 ms). A series of 200 volumes was acquired, resulting in a scan duration of 10:08 min.

### MRI data processing and statistical analysis

#### *Lesion mapping, voxel-based morphometry (VBM) and tractography*

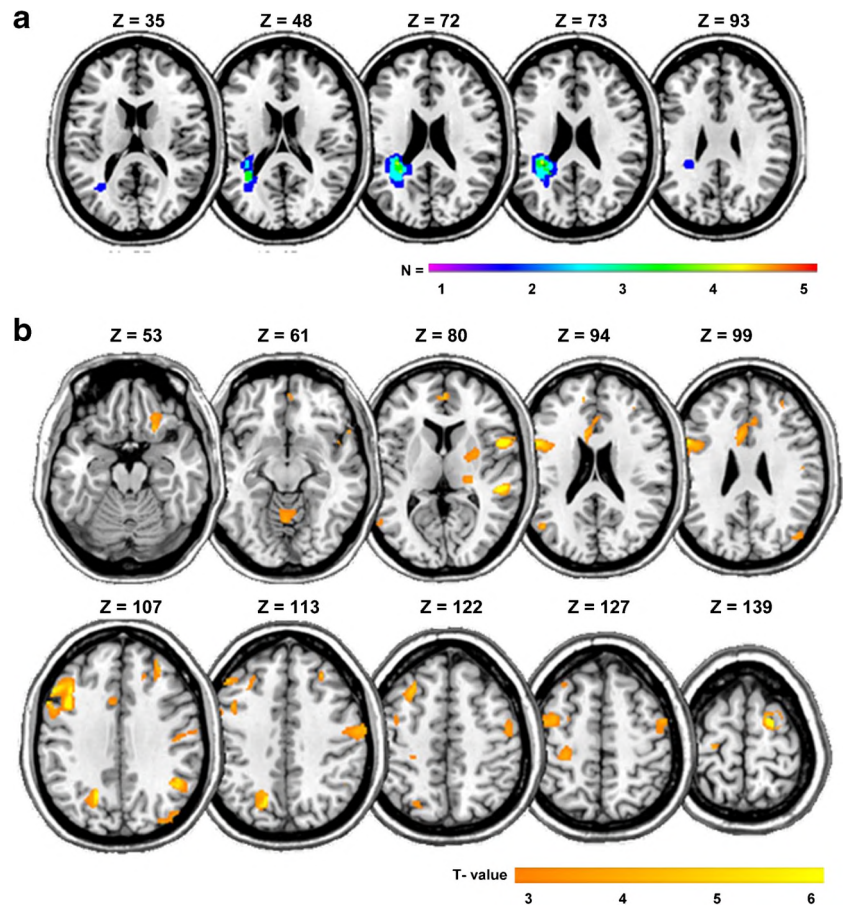
A lesion overlay was constructed to identify the voxels commonly affected by the lesion of interest in the MS+ patient group. Using MRICroN software (Rorden et al. 2007), T1-weighted hypointense WM lesion boundaries were manually delineated on the T1-weighted images of the patients after normalization to the T1 Montreal Neurological Institute (MNI) template. Figure 1a shows the lesion site within the posterior periventricular region (MS+ group). A common seed point for reconstructing the WM fibers affected by this lesion in the MS+ group was generated by creating a ROI centered on the peak overlap voxel. This was then used in DTI deterministic fiber tracking to determine the involved network regions. All DTI data were pre-processed using the SPM8 diffusion toolbox ([\[spmtools/\]\(http://www.sourceforge.net/projects/spmtools/\)\). Images were co-registered and re-sliced to the reference image acquired with  \$b=0\$  for motion correction. Tensor estimation and fiber tracking was performed using the MedINRIA DTI Track software \(<http://www-sop.inria.fr/asclepios/software/MedINRIA/>\) employing the streamline approach for tractography using angle and anisotropy thresholds of 0.2 and 0.3, respectively. Tractography was initiated employing the abovementioned ROI as a seed point and starting from its edges. The target termination point of these tracked WM fibers was determined as the endpoint of these fibers at the GM/WM boundary in the left parietal cortical regions, validated by superimposing them on the T1-weighted anatomical scans in subject-space \(see Table 2\). The subsequent rs-fMRI analysis was based on a seed ROI defined by the averaged cortical termination points of the WM obtained from the fiber tracking analysis.](http://www.sourceforge.net/projects/</a></p>
</div>
<div data-bbox=)

For the VBM analysis, a binary lesion map for each patient was first created based on the T1-weighted MPRAGE and T2-weighted FLAIR images using the lesion segmentation toolbox (LST) toolbox (Schmidt et al. 2012). Based on this lesion map, lesions on the T1-weighted images were filled. Using the VBM-8 toolbox (<http://dbm.neuro.uni-jena.de/>), the filled T1-weighted images were segmented and normalized to MNI space. The segmented GM and WM tissue probability maps were smoothed using an 8 mm kernel. Finally, a two-sample  $t$ -test was performed based on the segmented tissue probability maps to assess relative GM and WM atrophy across patient groups.

#### *rs-fMRI data processing and FC maps calculation*

rs-fMRI data sets were preprocessed using SPM8. For each subject, rs-fMRI volumes were re-aligned to the first volume image in order to correct for head movement. Then, the images were co-registered to the high-resolution anatomical scan. T1-MPRAGE images were then segmented to GM, WM and CSF probability maps. Normalization parameters obtained during the segmentation procedure were then applied to the re-aligned and co-registered rs-fMRI volumes. Finally,

**Fig. 1** **a** Lesion overlay map of the affected left posterior periventricular region in the  $n=5$  MS+ patients. The color scale indicates the overlap between delineated voxels affected by an MS plaque in these patients. **b** T-statistical map showing the detected differences in GM tissue density between both patients groups (MS+ vs. MS-). Significant reductions in GM are observed in the MS+ group in the following regions: right insular cortex, left inferior frontal gyrus, left precuneus, medial frontal gyrus (MFG), left temporal pole and right superior frontal gyrus (SFG) ( $p < 0.01$ , corrected)



rs-fMRI volumes were smoothed using an 8 mm kernel. After preprocessing, we used an in-house Matlab (Math Works, Inc.) script to extract the WM and CSF signal time-course using the WM and CSF masks defined by segmented tissue probability maps. The seed-region time course was extracted from a 6 mm radius spherical region-of-interest placed on the left precuneus seed point determined by tractography. In order to increase the statistical power for the group analysis, the data from other participants with a posterior periventricular lesion on the contralateral side (right side) was flipped through the x-axis, thus creating a group of  $N=5$  patients with a homogeneously affected left posterior periventricular site (MS+).

Resting state functional connectivity maps for all subjects were calculated using the REST toolbox (<http://restfmri.net/forum/index.php>). Network of interest (NOI) FC maps of

whole-brain voxel-wise correlation with the left precuneus seed region time course were generated. Raw data was band-pass filtered (0.08–0.1 Hz); the mean time courses for WM, CSF and head movement parameters were extracted and included as regressors in the design matrix to account for physiological noise. Fisher's correlation with z-transformation was calculated from the ROIs to whole-brain voxels.

#### Statistical comparisons

A flexible factorial design was used to test specific effects-of-interest, including time main effects in the whole group, as well as the group and time main effects in relation to the left parietal seed points between both MS+ and MS- groups.

For the single-case study, we used multiple regression analysis to test for changes in resting- state brain network in relation to the precuneus seed point over the investigated time period. Regressors-of-interest included both a linear and a quadratic contrast. The linear contrast tests if any brain regions show either increasing or decreasing FC relative to the seed point, whereas the quadratic contrast tests if any brain regions show a U-shaped (or inverted U-shaped) change of connectivity over the investigated time period. We assumed that the inverted quadratic contrast could be of particular interest since

**Table 2** Montreal neurology institute (MNI) coordinates of reconstructed LSF fibers affected by a left posterior periventricular MS lesion in the MS+ patients group

Patient code	MNI coordinates (X,Y,Z)
Pat_2	-14, -66, 46
Pat_4	-12, -68, 30
Pat_5	-10, -82, 32
Pat_6	-12, -74, 47
Pat_8	-12, -68, 30

it tests whether any brain regions show an initial elevation of FC levels following the lesion onset, and subsequently normalize to baseline levels as an indication to neural plasticity. The Fisher's correlation coefficients (Fisher's-Z) of the significant clusters from the regression analysis were extracted over the time course. The extracted Z-values across all follow-up sessions were then normalized in relation to the baseline levels (session 1) for each patient

$$(\Delta r = r_{(tx)} - r_{(t1)}, x = 2-5 \text{ for subsequent time points}).$$

A one-sample *t*-test was then carried out comparing the FC levels within these clusters over time in the whole MS group vs. the corresponding value from the single patient.

The overall significance level of all statistical comparisons (rs-fMRI and VBM) was determined based on Monte Carlo permutations, and corrected for multiple comparisons at the cluster level. This was accomplished using the AlphaSim algorithm based upon a combination of individual voxel-probability thresholding and spatial smoothing to generate a null distribution of random clusters. The minimum cluster size was then determined based on this null distribution. We used a statistical threshold of  $p=0.01$ , and based on a simulation of 10,000 permutations, the minimum extent threshold obtained for cluster size was found to be 248 voxels, corrected at a cluster alpha level of 0.05. Accordingly, all statistics reported in this paper adopt this criterion to control for multiple comparisons.

## Results

### Lesion mapping, VBM, and tractography

The MS+ group showed a significantly higher total lesion volume (TLV) ([mean±SD]  $6.24 \pm 3.9 \text{ m}^3$ ) compared to the MS- group ( $0.3 \pm 0.3 \text{ m}^3$ ), ( $T=2.9, p=0.023$ ). The voxels identified to be most commonly affected by left posterior periventricular lesions in the MS+ patients using lesion mapping are shown in Fig. 1a. Brain regions that showed significant GM tissue density reduction in the VBM analysis when comparing the MS+ vs. MS- groups are listed in Table 3a in MNI coordinates. Significant GM density reduction was detected in the right insular cortex, left inferior frontal gyrus, left precuneus, in both the left and right pre-central gyrus, left temporal pole, medial frontal gyrus (MFG) as well as in the right superior frontal gyrus (rsFG) in the MS+ group compared to the MS- group (Fig. 1b and Table 3a). No significant differences in WM were identified between the groups.

The tractography analysis reconstructed the left superior longitudinal fasciculus (LSF) as passing through the predilection site. The coordinates of the end points of the constructed network in the parietal cortex were obtained for each patient in

MNI space (Table 2). These termination point coordinates were averaged, creating a global seed point (center of mass: X, Y, Z:  $-12, -73, 38$ ) (Fig. 2) to be used for the subsequent voxel-wise Z-map calculation at the group level.

### FC maps statistical comparisons

#### *Longitudinal FC changes within the network of interest (NOI) in the whole patient sample*

According to the ANOVA conducted based on the five time points obtained for the whole patient group, there was no significant main effect of time ( $F=6, p>0.001$ , corrected for cluster size). Namely, no changes in FC levels were detected over time in the clinically stable RRMS patients.

#### *Between-group changes in FC*

The between-group (MS+ vs. MS-) ANOVA of the Z-maps at the follow-up sessions revealed a significant main effect of group. Higher FC levels were observed in the MS+ group compared to MS- in the brain regions adjacent to the rs-fMRI seed in the left precuneus. Moreover, higher FC levels were also observed in the contralateral regions extending from the right cuneus to the right precuneus regions in the MS+ group ( $T=5.12, p<0.0001$ , corrected for cluster size) (See Table 3B, and Fig. 3). Inclusion of age, disease duration or lesion load as covariates into the statistical model had no effect on the obtained results. Moreover, no significant Group\*Time interaction was detected ( $p>0.001$ , corrected for cluster size).

#### *Changes in brain FC following detection of new WM lesion (single case)*

Within the studied network of interest, changes in FC at rest were observed in a single RRMS patient who developed a new acute left posterior periventricular lesion in the second MRI follow-up session during the study (Suppl. Fig. 1). Based on the regression analysis ( $p \leq 0.01$ , corrected for cluster size), FC increases were observed in the right pre- and post-central gyri, right SMA, left cuneus, vermis and the posterior cerebellar lobe (Fig. 4a, *t*-values are listed in Table 3C). Figure 4b shows the baseline-corrected FC differences ( $\Delta r$ ) in the follow-up sessions ( $t_2-t_5$ ) within the identified clusters from the regression analysis for the whole MS group compared to those of the single-case patient.  $\Delta r$  values of the concatenated MS group were lower than those of the single patient in all clusters, and at all time points. The post-hoc one-sample *t*-tests showed significant differences in FC levels when comparing the single patient and overall MS group across the follow-up sessions. These significant differences are indicated in Fig. 4b (c.f. Suppl. Table 1 for *t*-values). Moreover, the time course of  $\Delta r$  for this individual patient demonstrated an inverted-U

**Table 3** Significant clusters identified in VBM analysis, rs-fMRI comparisons and the single-case study

Anatomical region	MNI coordinates (X,Y,Z)	Cluster size (# of voxels)	Z value	T value	P-value
a. Voxel based morphometry (VBM)					
Right insular cortex	53, 9, 6	763	4.85	12.9	0.013
Left inferior frontal gyrus	-42, 11, 37	2392	4.8	12.4	0
Left precuneus	-17, -64, 39	607	4.65	11.36	0.025
Superior frontal gyrus (SFG)	18, 0, 69	352	4.42	9.8	0.076
Left temporal pole	-32, 26, -33	806	3.5	7.91	0.01
Medial frontal gyrus (MFG)	-12, 51, 15	532	4	7.6	0.03
Left pre-central gyrus	-26, -24, 69	476	3.28	5.02	0.043
Right pre-central gyrus	50, -1, 54	830	3.26	4.97	0.01
b. Network of interest: between-group analysis					
Cluster extending from the right cuneus (BA-7) to the right precuneus	19, -72, 36 18, -60, 28	678	4.4	5.12	0
Left parietal lobe	-32, -48, 68	464	3.44	3.76	0
c. Single-case analysis: changes within network of interest over time following a new WM lesion					
Cluster extending from the right superior frontal gyrus (SFG) to the medial frontal gyrus (SMA)	10, -2, 78 -6, -10, 58	414	4.63	35.81	0
Left cuneus	-2, -98, 18	274	4.56	32.7	0
Right precentral gyrus	48, -8, 62	297	4.37	26.5	0
Vermis	-2, -72, -34	517	4.24	22.6	0
Cluster extending from the right post central gyrus to right precuneus	52, -32, 52 4, -58, 74	617	3.97	16.75	0
Cluster extending from the posterior cerebellar lobe to the anterior cerebellar lobe	-10, -62, -18	522	3.87	15.28	0

pattern over the investigated time course within all clusters. At t2 and t3 within these clusters,  $\Delta r$  values reached a peak ranging from 0.3 to 0.5 in all identified clusters. These  $\Delta r$  values were found to be higher compared to those observed in the later follow-up sessions. In t4 and t5,  $\Delta r$  levels within these clusters were observed to decrease to levels in the range 0–0.2 (Fig. 4b).

## Discussion

In MS, it is increasingly acknowledged that structural damage at and beyond the sites of inflammatory lesions as well as changes in brain connectivity patterns are features of the

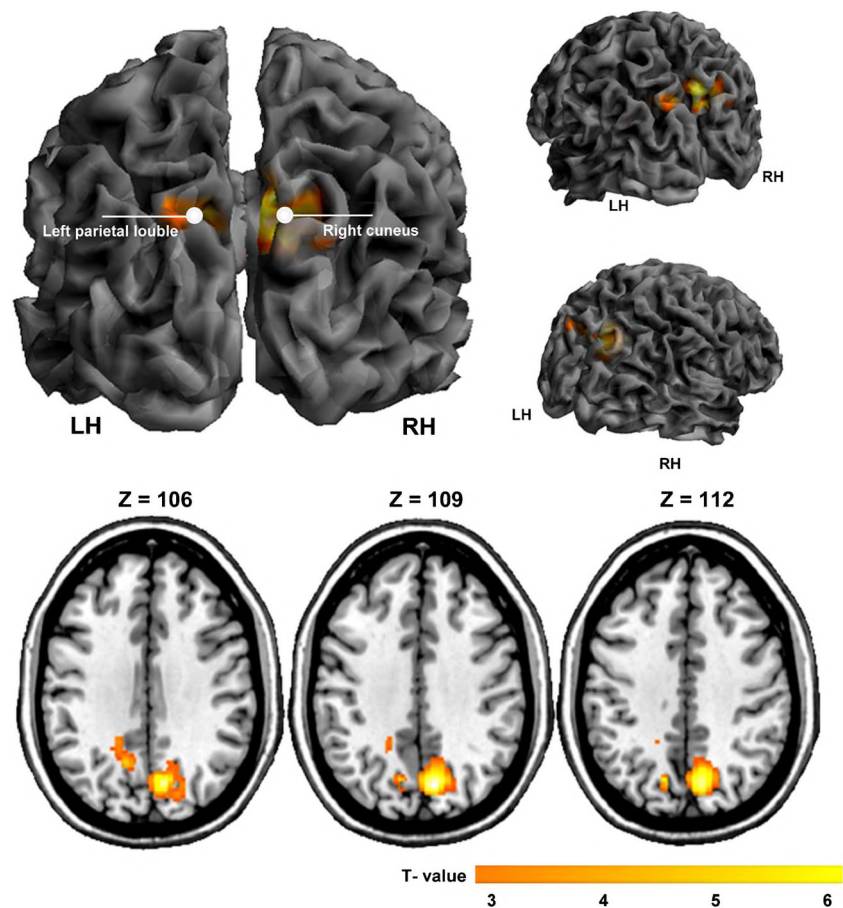
disease pathology. However, little is known about the impact that acute and chronic lesions have on global network connectivity. We investigated a group of RRMS patients using rs-fMRI with the goal of elucidating the longitudinal effects resulting from MS lesions located at predilection sites on FC patterns. We were able to demonstrate that over a stable disease course FC levels remain relatively unchanged within the investigated NOI, whereas in a single patient experiencing an acute relapse, a marked increase in FC was observed as a result of a newly developed WM lesion, indicative of the recruitment of intact brain regions.

In order to calculate the FC maps, we first performed tractography and VBM analyses to determine the cortical regions directly affected by the left posterior periventricular

**Fig. 2** Illustration of the tractography-defined seed point used (*red sphere*) for rs-fMRI analysis in MNI space (-12, -73, 38), relative to which Fisher's Z FC maps were calculated



**Fig. 3** Between-group differences in resting state FC in the precuneus network as a result of a single MS lesion (repeated measures ANOVA). Based on pairwise comparisons, a significant increase in FC is seen in the ipsilateral left precuneus as well as in the contralateral cuneus and precuneus regions in the MS+ group compared to MS- ( $p < 0.01$ , corrected)



lesion. Comparing the results of the VBM analysis for MS+ (patients with a predilection site lesion) to those of the MS- group, significant reductions in GM density were observed in the ipsilateral precuneus, inferior frontal gyrus (IFG), medial frontal gyrus (MFG) and temporal pole. Such GM density reductions have been previously associated with increased WM lesion volumes in RRMS (Louapre et al. 2014). This is consistent with reports that GM damage is driven by the accumulation of WM damage in RRMS, occurring via Wallerian degeneration mechanisms (Siffrin et al. 2010; Calabrese et al. 2015; Droy et al. 2015). Furthermore, the abovementioned brain regions are anatomically connected by the LSAF (Catani and Mesulam 2008), which is known to play a role in the symptoms of MS (Pujol et al. 2000).

The FC maps derived from the longitudinal rs-fMRI datasets acquired from RRMS patients revealed two main observations. Firstly, no changes in FC were observed over time in the whole MS patient group, pointing towards a preservation of FC in clinically stable RRMS patients within the studied precuneus network. Secondly, the between-group comparisons revealed a main effect of group, in which increased FC was observed in the ipsilateral parietal lobe (adjacent to the seed point) as well as in the contralateral cuneus and precuneus regions in the MS+ group. An increase in FC has

been reported to reflect adaptive compensatory mechanisms that serve to limit the clinical consequences of disease-related tissue damage (Filippi and Rocca 2010). Thus, the observed FC increase in the MS+ patient group may indicate recruitment of the intact adjacent and contralateral brain regions, compensating for damage resulting from the autoimmune attack in the posterior periventricular spaces.

Further evidence that compensation and cortical recruitment can be observed in early stages of MS has been reported in studies using both task-related and rs-fMRI (Reddy et al. 2002; Pantano et al. 2002; Basile et al. 2013). In a task-related fMRI study, RRMS and SPMS patients showed an increased bilateral activation of the motor cortex during both active and passive finger-tapping tasks; this increase in activation was found to correlate with the degree of clinical disability and the extent of microscopic brain tissue damage (Reddy et al. 2002). Similarly, Pantano et al. demonstrated that connectivity patterns of the motor cortex are altered following a single clinical relapse of MS, reporting that adaptive functional changes occur that involve both symptomatic and asymptomatic hemispheres (Pantano et al. 2002).

Using rs-fMRI, Basile et al. (2013) have examined both the SMN and DMN brain network components using rs-fMRI in MS patients and healthy controls (HC). The overall

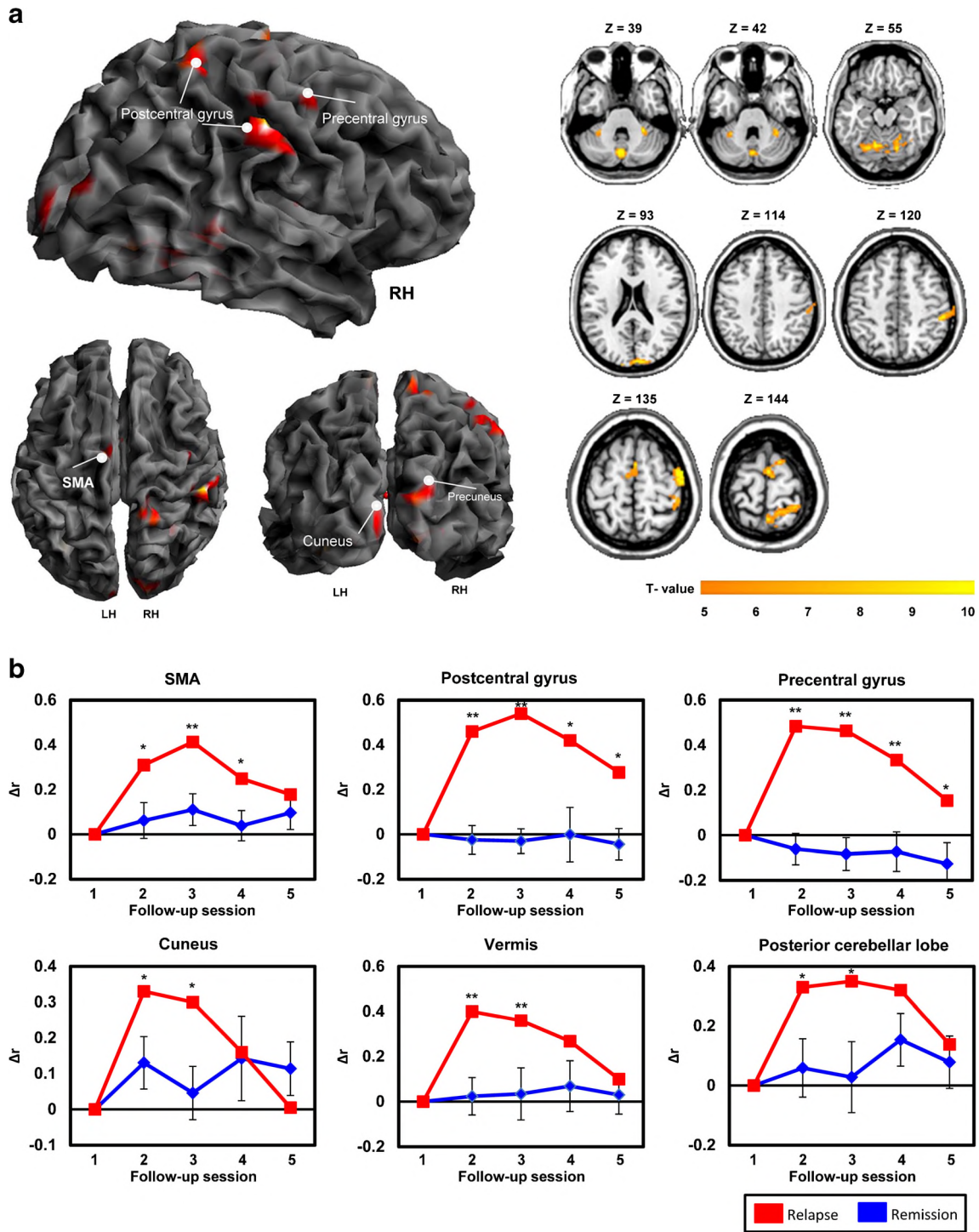


**Fig. 4** FC alterations over time in a single RRMS patient who showed a newly detected posterior periventricular lesion during the follow-up period. **a** T-statistical map based on the regression analysis of the FC maps obtained over 5 time points at 8 week intervals in this patient. An FC increase can be viewed in the right pre- and post-central gyri, SMA, left cuneus, the vermis and the anterior and posterior lobes of the cerebellum ( $p < 0.01$ , corrected). **b** These plots demonstrate the baseline-corrected FC differences ( $\Delta r$ ) in the follow-up sessions (t2–t5) within the identified clusters for the overall MS group in remission (blue lines) and the single-case patient after a relapse (red lines). As seen from the plots,

the average  $\Delta r$  values in the MS group were found to be lower than those of the single patient in all clusters and stable over time (blue bars, error bars denoting SEM). For the single patient (red bars), the  $\Delta r$  values showed an inverted-U pattern over the investigated time course within all clusters over the time period. Along the follow-up time period,  $\Delta r$  levels in these clusters were observed to decrease and finally normalize towards baseline levels. Significant differences in FC levels based on the pairwise post-hoc comparisons between the overall MS group and the single-patient across the follow-up sessions are denoted on the plots (single-sample- $t$ -test \*:  $p < 0.05$ ; \*\*:  $p < 0.001$ )

investigated group of MS patients showed areas of increased FC in both the SMN and DMN, whereas the subgroup of RRMS patients exhibited this only in the SMN. The authors concluded that at early stages of the disease when disability is minimal, the brains of RRMS patients tend to compensate for tissue damage by increasing FC in the non-dominant hemisphere.

Finally, we were able to investigate the spatial and temporal dynamics of FC levels prior and subsequent to an acute relapse in a single patient during the bi-monthly follow-up period relative to the precuneus seed point. In this patient, an increase in FC activation was found in the right pre- and post-central gyri, right SMA, left cuneus, vermis and the posterior cerebellar lobe. The time course of the Fisher's Z-values enclosed within these clusters was found to increase significantly in the acute phase. At later stages, the FC levels in these regions were observed to decrease. After the first MRI follow-up session, this patient experienced a clinical relapse, manifested as right-side optic neuritis (EDSS=2.5; at beginning of study, EDSS=1) and a new WM lesion affecting the posterior periventricular white matter. Over the following months, no further clinical or new Gd-enhancing WM lesions in MRI were detected. Our results indicate that compensation occurs in functional networks via inter-hemispheric connections following damage to the CNS in RRMS. Recruitment of inter-hemispheric connections between brain areas was also demonstrated in early MS patients using resting-state magnetoencephalography, where the authors reported an increase of connectivity levels in the bilateral occipital, temporal and parietal regions (Schoonheim et al. 2013). In MS, the degree of functional compensation depends on the integrity of these WM pathways, where neural compensation mechanisms were reported to be more likely to occur in the early stages of the disease, such as in RRMS patients (Basile et al. 2013), whereas in later stages of the disease, the extent of focal WM damage is more widespread (Siffrin et al. 2010).

Here, we were able to demonstrate that MS lesions affecting major WM pathways are capable of inducing widespread changes in network connectivity, possibly as a compensatory mechanism to minimize clinical consequences. Patients' fatigue might be a potential confounder in rs-fMRI studies, especially when studying MS populations. The included patients were in the early stages of MS with minimal cognitive deficits, and verbal reports of their alertness levels were obtained from patients following their scanning session. An additional limitation of this study is the small sample of patients. Larger studies are required to confirm our results and would be of particular interest for the investigation of the effects of other lesion predilection sites such as the brainstem and corpus callosum. A comprehensive understanding of neuroplasticity and neural reserve mechanisms in MS may eventually allow predictors for the disease course to be identified.

In conclusion, no significant fluctuations of FC levels were found in the whole patient group over the course of the study. However, in those exhibiting a chronic MS lesion occurring at an MS predilection site, increased FC was observed, predominantly in contralateral brain regions, which can be interpreted as the recruitment of intact cortical regions to compensate for ipsilateral tissue damage. Moreover, in one patient that developed a new lesion at the same predilection site during the study period, we observed temporary increases in FC in multiple regions, suggesting that initial recruitment and functional compensation occur during acute phases of the disease.

**Compliance with ethical standards** This study was performed in accordance with the ethical standards of the institutional and/or national research committee and with the 1964 Helsinki declaration and its later amendments or comparable ethical standards. Informed consent was obtained from all individual participants included in the study.

**Funding** This work has been supported by grants from the German Research Foundation (DFG; CRC-TR 128/B5 to Drs. Deichmann and Zipp).

**Conflict of interest** None of the authors declare any relevant conflicts of interest.

## References

- Basile, B., Castelli, M., Monteleone, F., Nocentini, U., Caltagirone, C., Centonze, D., Cercignani, M., & Bozzali, M. (2013). Functional connectivity changes within specific networks parallel the clinical evolution of multiple sclerosis. *Multiple Sclerosis*, *20*, 1050–1057.
- Bremel, R. A., & Naismith, R. T. (2015). Using MRI to make informed clinical decisions in multiple sclerosis care. *Current Opinion in Neurology*, *28*, 244–249.
- Calabrese, M., Magliozzi, R., Ciccarelli, O., Geurts, J. J. G., Reynolds, R., & Martin, R. (2015). Exploring the origins of grey matter damage in multiple sclerosis. *Nature Reviews Neuroscience*, *16*, 147–158.
- Catani, M., & Mesulam, M. (2008). The arcuate fasciculus and the disconnection theme in language and aphasia: history and current state. *Cortex*, *44*, 953–961.
- Ceccarelli, A., Rocca, M. A., Pagani, E., Colombo, B., Martinelli, V., Comi, G., & Filippi, M. (2008). A voxel-based morphometry study of grey matter loss in MS patients with different clinical phenotypes. *NeuroImage*, *42*, 315–322.
- Chard, D. T., & Miller, D. H. (2009). What you see depends on how you look: Gray matter lesions in multiple sclerosis. *Neurology*, *73*, 918–919.
- De Stefano, N., Narayanan, S., Francis, S. J., Smith, S., Mortilla, M., Tartaglia, M. C., Bartolozzi, M. L., Guidi, L., Federico, A., & Arnold, D. L. (2002). Diffuse axonal and tissue injury in patients with multiple sclerosis with low cerebral lesion load and no disability. *Archives of Neurology*, *59*, 1565–1571.
- Dogonowski, A. M., Siebner, H. R., Solberg-Sorensen, P., Wu, X., Biswal, B., Paulson, O. B., Dyrby, T. B., Skimminge, A., Blinkenberg, M., & Madsen, K. H. (2012). Expanded functional coupling of subcortical nuclei with the motor resting-state network in multiple sclerosis. *Multiple Sclerosis*, *19*, 559–566.
- Dogonowski, A.-M., Siebner, H. R., Soelberg Sørensen, P., Paulson, O. B., Dyrby, T. B., Blinkenberg, M., & Madsen, K. H. (2013). Resting-state connectivity of pre-motor cortex reflects disability in multiple sclerosis. *Acta Neurologica Scandinavica*, *128*, 328–335.

- Droby, A., Fleischer, V., Carnini, M., Zimmermann, H., Siffrin, V., Gawehn, J., Hildebrandt, A., Baier, B., & Zipp, F. (2015). The impact of isolated lesions on white matter fiber tracts in multiple sclerosis patients. *NeuroImage: Clinical*, 8, 110–116.
- Faivre, A., Rico, A., Zaaoui, W., Crespy, L., Reuter, F., Wybrecht, D., Soulier, E., Malikova, I., Confort-Gouny, S., Cozzone, P. J., Pelletier, J., Ranjeva, J. P., & Audoin, B. (2012). Assessing brain connectivity at rest is clinically relevant in early multiple sclerosis. *Multiple Sclerosis*, 18, 1251–1258.
- Filippi, M., & Rocca, M. A. (2010). MR imaging of gray matter involvement in multiple sclerosis: implications for understanding disease pathophysiology and monitoring treatment efficacy. *American Journal of Neuroradiology*, 31, 1171–1177.
- Filippi, M., Riccitelli, G., Mattioli, F., Capra, R., Stampatori, C., Pagani, E., Valsasina, P., Copetti, M., Falini, A., Comi, G., & Rocca, M. A. (2012). Multiple sclerosis: effects of cognitive rehabilitation on structural and functional MR imaging measures—an explorative study. *Radiology*, 262, 932–940.
- Fox, M. D., & Raichle, M. E. (2007). Spontaneous fluctuations in brain activity observed with functional magnetic resonance imaging. *Nature Reviews Neuroscience*, 8, 700–711.
- Gamboa, O. L., Tagliazucchi, E., von Wegner, F., Jurcoane, A., Wahl, M., Laufs, H., & Ziemann, U. (2014). Working memory performance of early MS patients correlates inversely with modularity increases in resting state functional connectivity networks. *NeuroImage*, 94, 385–395.
- Jones, D. T., Mateen, F. J., Lucchinetti, C. F., Jack, C. R., & Welker, K. M. (2011). Default mode network disruption secondary to a lesion in the anterior thalamus. *Archives of Neurology*, 68, 242–247.
- Louapre, C., Perlberg, V., Garcia-Lorenzo, D., Urbanski, M., Benali, H., Assouad, R., Galanaud, D., Freeman, L., Bodini, B., Papeix, C., Tourbah, A., Lubetzki, C., Lehericy, S., & Stankoff, B. (2014). Brain network disconnection in early multiple sclerosis deficits: an anatomofunctional study. *Human Brain Mapping*, 35, 4706–4717.
- Pantano, P., Iannetti, G. D., Caramia, F., Mainero, C., Di Legge, S., Bozzao, L., Pozzilli, C., & Lenzi, G. L. (2002). Cortical motor reorganization after a single clinical attack of multiple sclerosis. *Brain*, 125, 1607–1615.
- Polman, C. H., Reingold, S. C., Banwell, B., Clanet, M., Cohen, J. A., Filippi, M., Fujihara, K., Havrdova, E., Hutchinson, M., Kappos, L., Lublin, F. D., Montalban, X., O'Connor, P., Sandberg-Wollheim, M., Thompson, A. J., Waubant, E., Weinshenker, B., & Wolinsky, J. S. (2011). Diagnostic criteria for multiple sclerosis: 2010 revisions to the McDonald criteria. *Annals of Neurology*, 69, 292–302.
- Pujol, J., Bello, J., Deus, J., Cardoner, N., Marti-Vilata, J. L., & Capdevila, A. (2000). Beck Depression Inventory factors related to demyelinating lesions of the left arcuate fasciculus regions. *Psychiatry Research*, 99, 151–159.
- Reddy, H., Narayanan, S., Woolrich, M., Mitsumori, T., Lapierre, Y., Arnold, D. L., & Matthews, P. M. (2002). Functional brain reorganization for hand movement in patients with multiple sclerosis: defining distinct effects of injury and disability. *Brain*, 125, 2646–2657.
- Richiardi, J., Gschwind, M., Simioni, S., Annoni, J.-M., Greco, B., Hagmann, P., Schluep, M., Vuilleumier, P., & Van De Ville, D. (2012). Classifying minimally disabled multiple sclerosis patients from resting state functional connectivity. *NeuroImage*, 62, 2021–2033.
- Rocca, M. A., Valsasina, P., Absinta, M., Riccitelli, G., Rodegher, M. E., Misci, P., Rossi, P., Falini, A., Comi, G., & Filippi, M. (2010). Default-mode network dysfunction and cognitive impairment in progressive MS. *Neurology*, 74, 1252–1259.
- Rocca, M. A., Valsasina, P., Martinelli, V., Misci, P., Falini, A., Comi, G., & Filippi, M. (2012). Large-scale neuronal network dysfunction in relapsing-remitting multiple sclerosis. *Neurology*, 79, 1449–1457.
- Rorden, C., Karnath, H.-O., & Bonilha, L. (2007). Improving lesion-symptom mapping. *Journal of Cognitive Neuroscience*, 19, 1081–1088.
- Rovaris, M., Bozzali, M., Rodegher, M., Tortorella, C., Comi, G., & Filippi, M. (1999). Brain MRI correlates of magnetization transfer imaging metrics in patients with multiple sclerosis. *Journal of Neurological Sciences*, 166, 58–63.
- Rovira, A., Auger, C., & Alonso, J. (2013). Magnetic resonance monitoring of lesion evolution in multiple sclerosis. *Therapeutic Advances in Neurological Disorders*, 6, 298–310.
- Schmidt, P., Gasser, C., Arsic, M., Buck, D., Förschler, A., Berthele, A., Hoshi, M., Ilg, R., Schmid, V. J., Zimmer, C., Hemmer, B., & Mühlau, M. (2012). An automated tool for detection of FLAIR-hyperintense white-matter lesions in Multiple Sclerosis. *NeuroImage*, 59, 3774–3783.
- Schoonheim, M. M., Geurt, J. J. G., Landi, D., Douw, L., van der Meer, M. L., Vrenken, H., Polman, C. H., Barkhof, F., & Stam, C. J. (2013). Functional connectivity changes in multiple sclerosis patients: a graph analytical study of MEG resting state data. *Human Brain Mapping*, 34, 52–61.
- Siffrin, V., Vogt, J., Radbruch, H., Nitsch, R., & Zipp, F. (2010). Multiple sclerosis—candidate mechanisms underlying CNS atrophy. *Trends in Neurosciences*, 33, 202–210.
- Wojtowicz, M. A., Ishigami, Y., Mazerolle, E. L., & Fisk, J. D. (2014). Stability of intraindividual variability as a marker of neurologic dysfunction in relapsing remitting multiple sclerosis. *Journal of Clinical and Experimental Neuropsychology*, 36, 455–463.
- Zhou, F., Zhuang, Y., Gong, H., Wang, B., Chen, Q., Wu, L., & Wan, H. (2014). Altered inter-subregion connectivity of the default mode network in relapsing remitting multiple sclerosis: a functional and structural connectivity study. *PloS One*, 9, e101198.